The Neural Correlates of Conscious Vision

Delphine Pins and Dominic ffytche

Institute of Psychiatry, London SE5 8AF, UK

Conflicting accounts of the neurobiology of consciousness have emerged from previous imaging studies. Some studies suggest that visual consciousness relates to a distributed network of frontal and partietal regions while others point to localized activity within individual visual areas. While the two positions seem mutually exclusive, timing issues may help reconcile the two. Networks that appear unified in functional magnetic resonance imaging (fMRI) studies may reflect processes that are widely distributed in time. To help resolve this issue, we have investigated timing across a network correlating with consciousness in parallel fMRI and evoked potential (EP) studies of grating stimuli. At threshold, a stimulus is perceived on some occasions but not on others, dissociating sensory input and perception. We have found correlates of consciousness in the occipital lobe at 100 ms and in parietal, frontal, auditory and motor regions from 260 ms onwards. The broad temporal and spatial distribution of activity argues against a unified, distributed fronto-parietal correlate of consciousness. Instead, it suggests that correlates of consciousness are divided into primary and secondary network nodes, with early activity in the occipital lobe correlating with perception and later activity in downstream areas with secondary processes contingent on the outcome of earlier perceptual processing.

Introduction

In 1998, Crick and Koch outlined a strategy for the systematic investigation of consciousness (Crick and Koch, 1998). Their approach was to focus on a specific aspect of consciousness – visual consciousness – and to assume that, within the visual system as a whole, some neural activity would correlate with conscious visual experience while other activity would not. The challenge for neuroscience became one of disentangling the two classes of activity and interest was re-awakened in paradigms where, by design or misfortune, input to the visual system and perception became dissociated (perception is used here as a synonym for conscious visual experience). The rationale behind such experiments was that a change in cerebral activity could be used as a signature for conscious or non-conscious processing. In paradigms where visual input changed while perception remained constant, the changing neural activity revealed non-conscious cerebral processes. Conversely, in paradigms where input remained constant but perception changed, the changing neural activity revealed the neural correlates of consciousness.

While dissociation paradigms held much promise, in practice they have led to two conflicting neurobiological accounts of visual consciousness: one distributed, one localized. Lumer *et al.* (Lumer *et al.*, 1998), using a binocular rivalry paradigm, showed that perceptual transitions between two constant retinal stimuli correlated with activity in a fronto-parietal network of areas, the same network identified by Dehaene *et al.* (Dehaene *et al.*, 2001) comparing seen and unseen words in a masking paradigm. Such studies view visual consciousness as a correlate of activity within a network of frontal and parietal areas. Other studies have argued for a correlate of consciousness in which fronto-parietal networks play no part. Zeki and ffytche (Zeki and ffytche, 1998) showed that the difference between seeing and not seeing visual motion in patient GY was the level of activity within a single visual area – area V5. In support of this localized view, percepts without sensory input (visual hallucinations) and visual illusions correlate with increased activity within single visual areas (ffytche and Zeki, 1996; ffytche *et al.*, 1998). Such studies suggest multiple independent correlates of consciousness, localized within individual cortical areas and contributing to consciousness as and when required (Zeki and Bartels, 1998; ffytche, 2000).

Given that the relationship between brain and mind is unlikely to change from one paradigm to another, one is left wondering why the correlates of visual consciousness differ in the studies reported above. Does the inconsistency imply that one or other of the views is wrong or might there be a way of reconciling the two? One possibility is that the differences result from a fundamental weakness in PET and fMRI imaging techniques – their lack of temporal resolution. Activity that might appear as a single spatially distributed network when imaged by fMRI or PET could, in fact, be distributed in time over several seconds. A temporal offset between perception and activity within parietal or frontal network nodes would weaken the case for a unitary distributed correlate of consciousness. Conversely, simultaneous activity distributed across a fronto-parietal network and coincident with perception would strengthen it. We have explored this issue further in parallel functional magnetic resonance imaging (fMRI) and evoked potential (EP) studies of a visual threshold detection task. At threshold, the same stimulus is perceived on some occasions but not on others, providing a dissociation between visual input and visual percept. By comparing the cerebral activity for trials in which subjects saw the stimulus with those in which they did not, we hoped to characterize both the timing and location of the neural correlates of visual consciousness.

Materials and Methods

Subjects

Twelve volunteers (seven males; mean age 28 years, range 21–38 years; 10 right-handed) took part in the study (two of them were the authors). All had normal corrected vision (two wore fMRI compatible corrective lenses during the fMRI scan). Subjects participated in task training, EP and fMRI sessions over a period of, on average, 5 weeks. One subject was unable to tolerate the fMRI scan and withdrew from the study. Five of the remaining 11 subjects took part in a parallel EP session. The study was approved by the Institute of Psychiatry Ethical Committee (Research), and was undertaken in compliance with the safety guidelines for MR research.

Stimuli

The stimulus consisted of a circular, sinusoidal grating of ~1 cycle/degree

appearing on a grey background and subtending 7.2° of visual angle in the centre of the visual field. The mean luminance of the grating was 3.5 cd/m^2, with a contrast of 1.3% ($L_{max} - L_{min}/L_{max} + L_{min}$). Background luminance was equal to the mean luminance of the stimulus. A small grey cross in the centre of the screen served as a fixation mark to minimize eye movements. For training and EP sessions the stimulus was presented on a computer monitor (Mitsubishi, 72 Hz refresh rate, screen–eye distance 45 cm). In the fMRI environment, it was back-projected onto a translucent screen placed at the end of the scanner bore and viewed through an angled mirror (LCD video projector; 72 Hz refresh; screen–eye distance 1.80 m). The spatial frequency and subtended visual angle of the grating was the same in training, EP and fMRI sessions. A subset of subjects were also presented the stimulus at an eccentricity of 7.2°. The eccentricity experiments will not be discussed further as only two subjects had eccentric EPs recorded, limiting the timing conclusions that could be drawn.

Threshold Stimulation

In order to maximize the power of our fMRI and EP statistical tests, we needed to obtain an approximately equal number of trials in which the grating had been seen and not seen (a 50% detection threshold). To achieve this, we used a modified version of the threshold estimation procedure described by Levitt (Levitt, 1971), varying the duration of the grating from trial to trial based on the subject's response. Two descending staircases were run, randomly interleaved. Within each staircase, the duration of a trial decreased by ~14 ms (one screen refresh; 1/72 Hz) for a 'Yes (I saw something)' response and increased by ~14 ms for a 'No (I did not see something)' response. Stimulus duration was changed in steps of 70 ms at the start of each experiment until the first response inversion to allow subjects to reach the threshold region in fewer trials. The advantage of the method was that subjects would remain at a 50% detection rate, even if their concentration or vigilance fluctuated during the course of an fMRI or EP session. In the subsequent analyses, threshold grating duration was defined as the mean stimulus duration ± 1 SD (the first 10 trials of each experiment were discarded before calculating the mean and SD).

Stimulation Protocol

Subjects were asked to fix the cross throughout the experiment. Each trial consisted of an initial sound prompt, the presentation of the grating, and a response sound prompt (see Fig. 1). The two sound prompts were different to avoid confusing trial start and end. The first sound was followed by the grating after a delay of 550 ms (pre-stimulus time) + 0–1100 ms (random time). The random time ensured that subjects could not anticipate when the stimulus was to appear. The presentation of the grating was followed by a 550 ms delay (post-stimulus time) before the response prompt. The duration of the grating and the timing of its presentation changed from trial to trial; however, by adjusting the post-stimulus time, the overall trial time remained constant. Subjects were required to press one of two buttons with the right hand to indicate 'Yes, I saw' or 'No, I did not see' the grating. Half the subjects used their right index finger for the 'Yes' responses, the other half for 'No' responses to control for differences in the motor representation of each finger. Different timing parameters were used for training, fMRI and EP sessions. In fMRI sessions, an inter-trial interval of 13.56 s allowed the haemodynamic response to return to baseline between trials. In training and EP sessions, the inter-trial interval was decreased to 3.3 s and 1.41 s, respectively. In the EP session, the pre- and post-stimulus times were decreased to 200 ms and the random time to 0–450 ms, to allow the acquisition of more trials within the same time period. The initial grating duration was set at 500 ms for training sessions and 240 ms for fMRI and EP sessions. For four subjects in the EP experiment and two subjects in the fMRI experiment, Catch trials (in which no grating was presented) were pseudo-randomly distributed throughout the experiment.

Experimental Protocol

Before each experiment, subjects were dark adapted and performed a brief threshold estimate. Brief threshold estimates were identical to the threshold experiments except that, instead of continuing for a fixed number of trials, they stopped after 10 response inversions (threshold was defined as the mean duration of the last 10 trials). Training was undertaken in three sessions and consisted of six (divided across the three sessions) brief threshold estimates and practice experimental runs with longer inter-stimulus intervals. In fMRI sessions each experiment

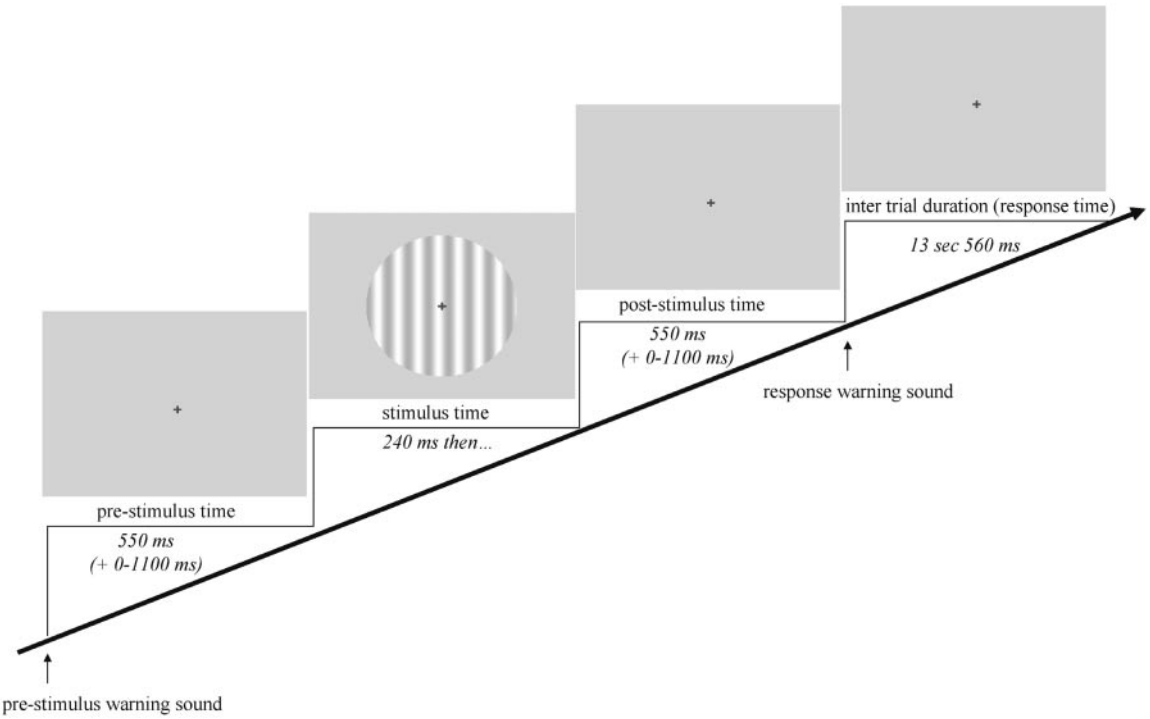

Figure 1. Time course of a trial for the fMRI experiment. A warning sound was followed by the grating after a pre-stimulus time of 550 ms (plus a random time of 0–1100 ms). A second sound (response prompt) appeared after a post-stimulus time of 550 ms (plus the remainder of the random time). Subjects gave their responses after the response prompt and waited for the next trial (inter-trial interval 13.56 s). The same trial design was used for training and EP sessions with different timing parameters.

contained 70 trials which, in two of the subjects, included 15 Catch trials (total duration 18 min 32 s). In EP sessions, the experiment was performed twice, each repeat containing 240 trials including 50 Catch trials (duration of each experiment 10 min). The response evoked by a supra-threshold, high contrast (76%) grating was also recorded in the EP session (100 trials, grating duration fixed at 240 ms).

fMRI Acquisition and Analysis

Scanning Protocol

Functional images were acquired on a 1.5 Tesla GE Neuro-optimized Signa LX Horizon System (General Electric, Milwaukee, WI, USA) equipped with an advanced NMR operating console and quadrature birdcage for radiofrequency transmission and reception. A gradient echo planar sequence (Kwong *et al.*, 1992) sensitive to blood oxygenation level dependent (BOLD) contrast was used (T_R = 2 s; T_E = 40 ms, flip angle = 90°, 64 × 64 matrix, in-plane voxel size = 3.75 × 3.75 mm, in a 24 cm field of view). Sixteen axial slices, parallel to the plane passing through the anterior and posterior commissures (AC-PC), were acquired every 2 s (7 mm thick with 0.7 mm interslice gap). This resulted in eight MR volumes with whole brain coverage for each trial. The 16 slices were acquired as two interleaved eight slice volumes, each lasting 1 s, minimizing offsets in sampling time between different brain regions. The first four volumes were discarded leaving a total of 556 volumes for each experiment. A high-resolution structural scan was acquired after the experiment consisting of 124 axial slices, 1.5 mm thick (SPGR sequence; T_R = 16 ms, flip angle = 20°, 256 × 256 matrix, in-plane voxel size = 0.859 × 0.859 mm, T_E = 5 ms, T_I = 300 ms). The timing of stimulus presentation was synchronized with scan acquisition using a TTL pulse from the scanner at the start of the experiment.

Image Pre-processing

For each subject, the 556 volume functional time series was motion corrected (Friston *et al.*, 1996a), transformed into stereotactic space and smoothed in x, y and z with a 6 mm full width half maximum (FWHM) Gaussian filter using SPM99 (Wellcome Department of Cognitive Neurology, London, UK, http//www.fil.ion.ucl.ac.uk/spm), implemented in Matlab (Mathworks Inc., Sherborn, MA). The activity at each voxel was scaled, high pass filtered and temporal autocorrelations removed (Friston *et al.*, 2000).

Modelling Activations and Suppressions

The functional time series were analysed using fixed and random effect models. Fixed effect models are more sensitive than random effect models when effect size and subject numbers are small (Friston *et al.*, 1999); however, unlike random effect models, they may be biased by unrepresentative subjects. In order to maximize our sensitivity and protect against bias we used a combined approach, testing for effects with a stringent statistical threshold in a fixed effect model and confirming that the activations were representative of the population as a whole using a random effect model at a lower threshold. The fixed effect model consisted of a series of stick functions coincident with the start of each trial and convolved with the haemodynamic response function. For each subject, three covariates were modelled: one for trials with 'Yes' responses at threshold, one for trials with 'No' responses at threshold and one for non-threshold trials (a fourth covariate was included to model Catch trials in the two subjects tested with this condition). Parameter estimates for each covariate were tested for: (i) activations from baseline (ii) suppressions from baseline. The random effect model consisted of a one sample *t*-test of each subject's 'Yes' contrast image. Activations or suppressions in the fixed effect model were considered significant at $P < 0.05$ corrected for multiple comparisons at the voxel level (Friston *et al.*, 1996b). Activations or suppressions in the random effect model were considered significant at $P < 0.01$ uncorrected.

Modelling Differential Activations and Suppressions

Differences between Yes and No trials were too small to be detected at a corrected level of significance even in the more sensitive fixed effect analysis. We therefore adopted a region of interest approach to explore the data further. Parameter estimates for Yes and No trials were tested for (i) differences in activation within voxels significantly activated for Yes trials in the analysis described above (ii) differences in suppression within voxels significantly suppressed for Yes trials in the analysis described above. Differential activations or suppressions were considered significant at $P < 0.05$ uncorrected within the regions of interest.

EP Acquisition and Analysis

EEG and eye movement activity was recorded using a 32 channel SYNAMP system (Neuroscan, Sterling, VA) and a Ag/AgCl 32 channel QuikCap with a linked mastoid reference (NeuroMed, Sterling, VA). The location of each recording electrode is shown in the inset in Figure 5*a*. EEG data were digitized at 1 kHz with a resolution of 0.084 μV/LSB and band pass filtered from 0.3 to 30 Hz. Electrode impedances were maintained below 5 kΩ. Triggers from the stimulus computer marked the timing of auditory prompts, grating onset/offset and motor response. Off line analysis was performed using SCAN v. 4.1 and v. 4.2 software (Neuroscan). Eye blinks were removed using the automated ocular artefact reduction module in SCAN. The EEG for each subject was epoched around the following events of interest: (i) auditory warning signal (ii) grating onset, (iii) auditory response signal and (iv) motor response. Epochs contaminated by subject movement or dominated by alpha activity were discarded. In order to bias the EEG to local cortical sources (Gevins, 1987) the EEG was transformed into a Laplacian derivation by comparing the activity at each electrode with its four immediate neighbours. Yes, No and Catch trial epochs were averaged for each subject to produce a subject-specific EP for each event of interest and each trial category. The subject-specific averages were pooled to make inter-subject average responses for each event and category (10 subject-specific averages for each inter-subject average – 5 subjects × 2 repeats). For P100, N2, P3, CNV, auditory N1 and motor N2-P2 components, the electrode displaying maximal amplitude was identified and the difference in amplitude of Yes and No trials compared with a paired *t*-test. Each experiment was treated as an independent estimate of response amplitude resulting in 10 paired comparisons. To investigate alpha power, epochs time locked to the first sound prompt were convolved with a Hanning window, transformed into the frequency domain (~1 Hz resolution) and divided into Yes, No and Catch trials. Alpha power at PZ for Yes and No trials was compared with a paired *t*-test.

fMRI and EP Integration

We used both qualitative and quantitative approaches to the integration of EP and fMRI data. The qualitative approach matched fMRI activations or suppressions with EP components based on (i) their location and (ii) the influence of trial category. Quantitative source modelling techniques were employed to compare the scalp topographies of occipital fMRI activation foci. A three-sphere model was used with spherical shell conductivities of 0.33, 0.0042 and 0.33 S/m.

Results

Psychophysics

Threshold Stability

Training sessions facilitated stable psychophysical performances across fMRI and EP sessions (see Fig. 2*a*; training session last threshold estimate: 54.72 ± 36.03 ms; fMRI session: 50.32 ± 23.98 ms; EP session: 62.21 ± 58.73 ms; repeated measures ANOVA: $F < 1$, NS). Threshold was not influenced by the variation in inter-trial duration between fMRI, EP and training sessions (mean threshold for short inter-trials: 40.83 ± 24.46 ms; mean threshold for long inter-trials: 43.13 ± 24.48 ms; paired *t*-test: $t(11) = -1.198$, NS). During fMRI and EP experiments, subjects reached a threshold level within 10 trials and remained there without significant fluctuations for the remaining trials (see Fig. 2*b* and 2*c*; repeated measures ANOVA fMRI: $F < 1$, NS; repeated measures ANOVA EP: $F < 1$, NS). Subjects made few 'Yes' responses to Catch trials (0–6% of Catch trials), precluding formal estimation of the d' and β

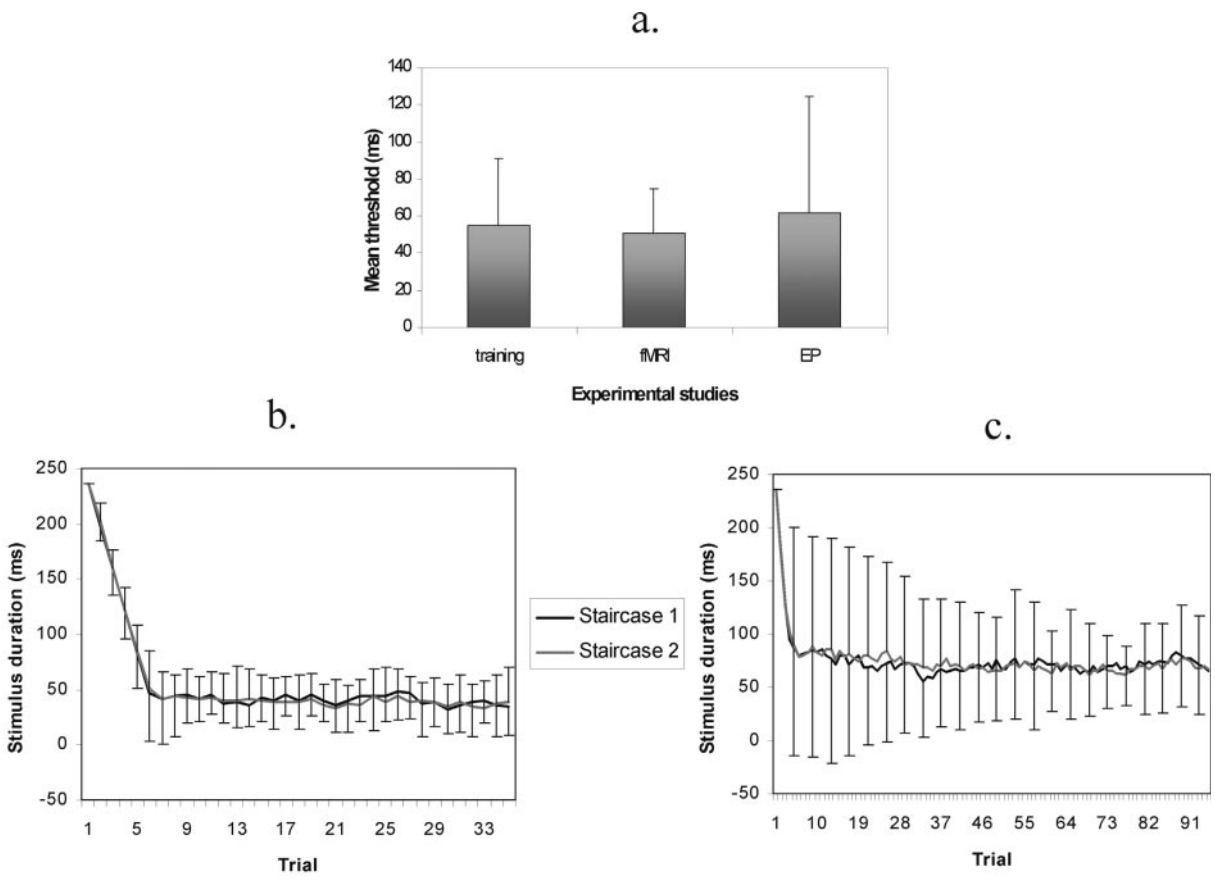

Figure 2. (*a*) Mean brief threshold estimate (+ SD) in training, fMRI and EP sessions. The threshold was not affected by the differences in recording environment. (*b*) Mean (±SD) grating duration for each trial in the fMRI session. (*c*) Mean (±SD) grating duration in the EP session. Subjects reached a threshold level within the first 10 trials of both sessions.

parameters of signal detection theory but indicating a stringent response criterion (Green and Swets, 1966).

Dissociations at Threshold

The threshold estimation procedure produce an approximately equal number of 'Yes' and 'No' responses for subsequent analysis (fMRI sessions: Yes = 27 ± 8% of trials; No = 28 ± 8%; EP sessions: Yes = 26 ± 6%; No = 26 ± 5%). Our definition of the threshold stimulus duration (mean ± 1 SD) resulted in a single duration value being used for some subjects and a 13–27 ms range of durations for others. In EP experiments, stimulus duration for Yes and No trials was not significantly different [mean duration 'Yes' trials: 67.53 ± 63 ms; 'No' trials: 62.36 ± 60 ms; paired *t*-test: $t(4) = -2.46$, NS]. In fMRI experiments there was a small but significant bias with longer stimulus durations associated with Yes trials and shorter ones with No trials [mean duration 'Yes' responses: 44.53 ± 22 ms; 'No' responses: 38.37 ± 19 ms; paired *t*-test: $t(10) = -4.12$, $P < 0.003$].

fMRI

Activations and Suppressions for Yes Trials

A network of brain regions corresponding to visual, motor and auditory systems were activated for Yes trials (Fig. 3 and Table 1). Visual activations were found in the thalamus, striate cortex, fusiform gyrus, medial occipital lobe (see also Fig. 4). In general, visual activations were symmetrical but only exceeded the stringent statistical criteria in one hemisphere (sub-threshold activations at the equivalent locations in the opposite hemisphere are also shown in the table). In the motor system, activations were found within left sensorimotor cortex and right cerebellar hemisphere, corresponding to the right hand button press, and the supplementary motor cortex in both hemispheres (resulting in an activation cluster spanning the midline). In the auditory system, activations were found in the superior temporal gyrus bilaterally. Activations were also found bilaterally in the insula. Areas of suppression were found bilaterally in the supra-marginal gyrus (parietal), the posterior cingulate and parahippocampal gyrus (limbic) and in an extended region passing from the superior frontal sulcus through the medial frontal gyrus to the anterior cingulate gyrus (frontal).

Differences Between Yes and No Trials

The images on the left of Figure 3 show that the areas activated (or suppressed) during Yes trials were also activated (or suppressed) during No trials. A subset of these regions showed a significant difference in response (see Table 1 and right of Fig. 3). In the visual system, V1, the medial occipital lobe and right LO were more active for Yes than No trials whereas the response in the fusiform gyrus, thalamus and left LO was no different for the two trial categories (see Fig. 4*a*). In addition to visual areas, sensorimotor cortex, cerebellum, posterior supplementary motor area and left auditory cortex showed Yes > No activations. Differential Yes > No suppressions were found in the posterior cingulate gyrus and in the swath of suppression extending from the superior frontal sulcus region to the anterior cingulate gyrus.

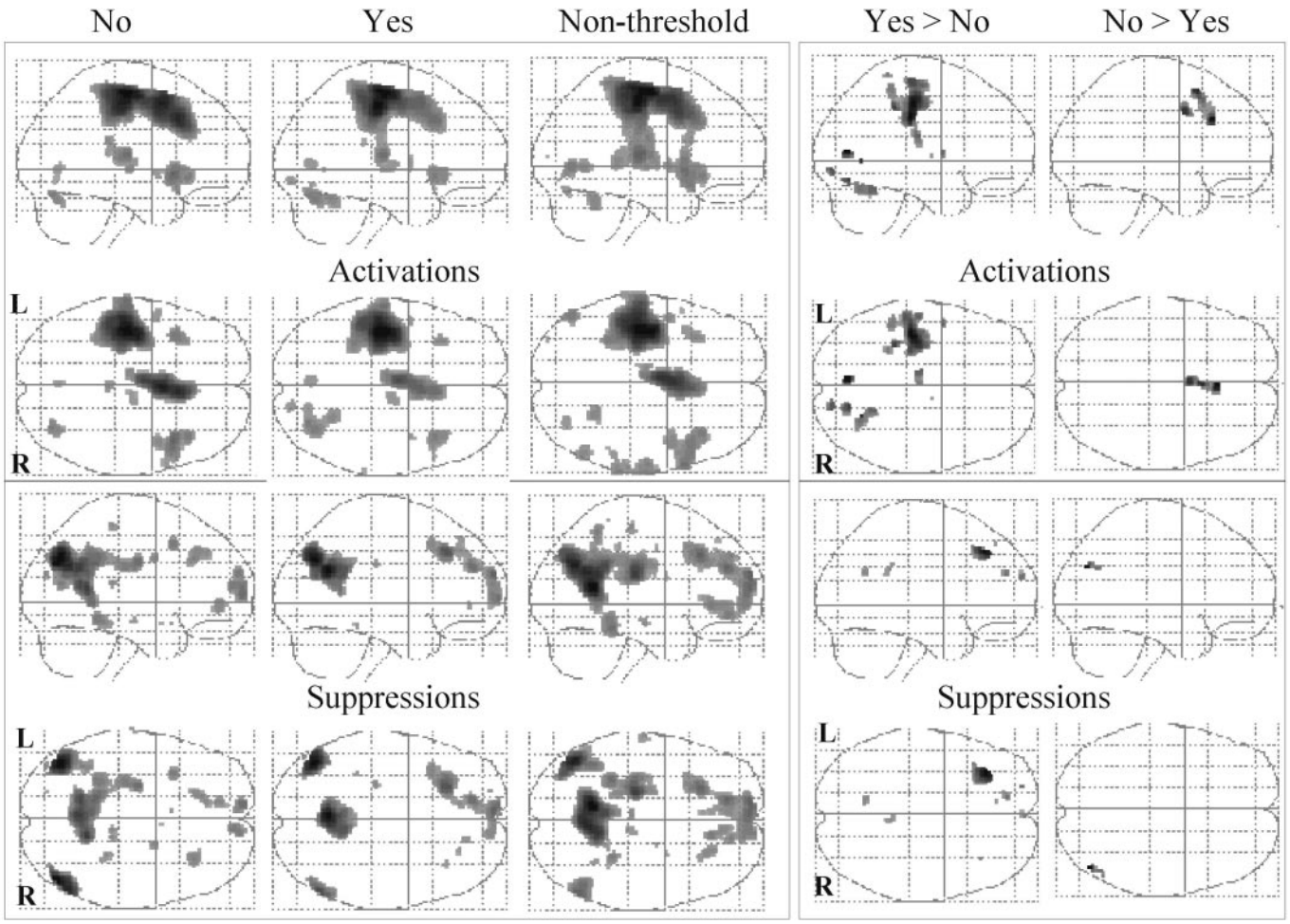

Figure 3. The left of the figure shows fMRI activations and suppressions for No, Yes and non-threshold trials in the fixed effect model. Two 'glass brain' views are displayed for each condition (upper image = viewed from side; lower image = viewed from above). The images have been thresholded at $P < 0.05$ corrected for multiple comparisons at the voxel level. Consistent responses are shown across the three trial categories. The right of the figure shows regions differentially activated or suppressed by Yes and No trials at $P < 0.05$ uncorrected within the region of interest defined by Yes trials.

Range versus Single Value Threshold

Since the psychophysical data indicated a response bias in the fMRI session with longer stimulus durations related to Yes responses and shorter stimulus durations to No responses (see above), we re-examined the fMRI results using a single stimulus duration for each subject. The single value analysis had the disadvantage of decreasing the number of threshold trials from 55% to 24% of all trials presented, with a consequent loss of statistical power. However, the pattern of results obtained from the single value model was the same as that in the range model. Of particular importance is the fact that, even with the lowered statistical power of the single value model, right V1 and right LO showed a significant differential increase in activity for Yes trials compared with No trials (Fig. 4*b*).

Evoked Potentials

Several neurophysiological components were evoked by the task, each differing in their timing, scalp distribution and relationship to task category. We will describe each of them in turn.

Early Components

The high contrast supra-threshold grating evoked a series of positive and negative waves over the occipital and parietal lobes (Fig. 5). The scalp distribution of the first positive wave, peaking at 100 ms (P100), exhibited two maxima, one over the lateral surface of each occipital lobe. The distribution of the negative wave peaking at 180 ms (N180) was anterior and superior to P100 and extended over the midline. The final positive wave peaking at 250 ms (P250) had the same topography as N180. The threshold grating evoked a P100 for Yes trials but not for No trials with the same bilateral distribution as the P100 for high contrast gratings [Fig. 6 – P100 amplitude Yes > No trials: $t(9) = 3.849$, $P < 0.01$].

Intermediate Latency Components

Yes trials elicited a negative wave at 260 ms with a left parietal maximum in the Laplacian transformed data (see Fig. 6). We have labelled the wave N2 because its latency is similar to the N2 wave found in visual oddball tasks [295 ± 43 ms (Simson *et al.*, 1977a); 240 ± 16 ms (Onofrj *et al.*, 1990)]. N2 was larger in amplitude for Yes than No trials [$t(9) = 3.921$, $P < 0.01$] and was followed by a positive wave peaking at 450 ms. The early part of this positive wave was characterized by bilateral maxima over each frontal lobe (P3a); the later part by bilateral maxima in the parietal lobe (P3b). P3a responses were significantly larger for

Table 1
Generic activations and suppressions for Yes trials

			Differential responses	Voxel level (*T*)	Talairach coordinates		
					x	*y*	*z* (mm)
Activations							
Visual activations	fusiform gyrus	L[a]		4.12	–30	–72	–14
		R		6.38	30	–74	–20
	thalamus	L		4.60	–8	–16	2
		R		5.57	10	–12	4
	LO	L[a]		3.42	–36	–84	4
		R[a]	Y > N	4.52	32	–88	4
	medial occipital lobe	L	Y > N	5.38	–4	–72	4
		R[a]	Y > N	4.09	10	–76	4
	V1 pole	L[a]	Y > N	4.39	–8	–92	–6
		R	Y > N	5.51	16	–88	–8
Motor activations	sensorimotor cortex	L	Y > N	13.72	–42	–18	58
	suppl. motor area posterior		Y > N	4.72	–12	–16	44
	suppl. motor area anterior		N > Y	5.31	4	24	32
	cerebellum	R	Y > N	5.83	24	–56	–24
Auditory activations	auditory cortex	L	Y > N	7.29	–60	–18	12
		R		4.82	66	–34	20
Miscellaneous activations	insula	L		5.95	–34	24	–2
		R		6.62	40	18	–4
	insula 2	L	Y > N	5.22	–48	0	6
Suppressions							
Parietal suppressions	supramarginal gyrus	L		7.91	–44	–70	34
		R	N > Y	6.46	54	–66	26
Limbic suppressions	posterior cingulate gyrus	L	Y > N	8.04	–2	–60	24
		R		7.29	2	–60	24
	parahippocampal gyrus	L		4.76	–36	–38	–18
		R[a]		4.16	26	–38	–20
Frontal suppressions	superior frontal sulcus	L	Y > N	6.32	–24	28	40
		R	Y > N	4.87	34	28	40
	medial frontal gyrus	L	Y > N	5.90	–8	64	22
		R	Y > N	5.21	10	62	22
	anterior cingulate gyrus	L		4.75	–12	44	–4
		R[a]		3.92	8	48	–2

Threshold $P < 0.05$ corrected fixed effect model and $P < 0.01$ uncorrected random effect model. Differential responses within regions of interest defined by the Yes trial response at $P < 0.05$ uncorrected fixed effect model.

[a] $P < 0.001$ uncorrected fixed effect and $P < 0.05$ uncorrected random effect model.

Yes trials than No trials over both hemispheres [P3a left: $t(9) = 3.947$, $P < 0.01$; P3a right: $t(9) = 2.482$, $P < 0.05$]. P3b responses were significantly larger for Yes than No trials over the right but not the left hemisphere [P3b left: $t(9) = 1.732$, NS; P3b right: $t(9) = 3.060$, $P < 0.02$].

Late Components
A negative slow wave was present for Yes trials but not No or Catch trials, maximal over the left parietal lobe [see Fig. 7; $t(9) = 3.789$, $P < 0.01$]. It followed the P3b wave (see Fig. 6) and was maximal 200 ms before subjects pressed the response button.

Motor and Auditory Evoked Potentials
The sound prompts for the start and end of each trial elicited a negative (N1) positive (P2) wave sequence, maximal over the vertex and temporal electrodes, which differed in timing for the two sounds (see Fig. 8). The N1 responses for the pre-stimulus sound were identical for Yes and No trials [$t(9) = 0.673$, NS]. The N1 response for the second sound was larger for Yes than No trials over left auditory cortex [$t(9) = 3.892$, $P < 0.01$]. Motor activity was associated with a negative (N2) wave and positive (P2) wave in the left fronto-central region with simultaneous inverted waves in the left parieto-central region (Fig. 7). The phase reversal from left fronto-central to left parieto-central regions is consistent with a generator in the left sensorimotor cortex. N2/P2 amplitude was greater for Yes than No trials [$t(7) = 3.744$, $P < 0.005$, $n = 8$ due to electrode fault in one subject].

Eye Movements
Subjects maintained fixation for the duration of each trial. On average, blinks occurred 500 ms after the presentation of the grating. While eye movements were not recorded during the fMRI session, there is no reason to suggest that subjects would have had different eye movement behaviour in the fMRI environment.

Discussion

We set out to identify the neural correlates of consciousness by presenting a grating at threshold and comparing trials in which subjects reported seeing it with those in which they did not. Using fMRI, we found differential responses for Yes and No trials in visual, motor, auditory, parietal, limbic and frontal regions. Taken by themselves, the results would have led us to conclude that the neural correlate of consciousness involved a distributed network. However, our parallel EP measures showed that the differences between Yes and No trials varied in their timing. Below we integrate the fMRI and EP evidence and, in doing so, reveal something of the timing and location of neural processes related to perception.

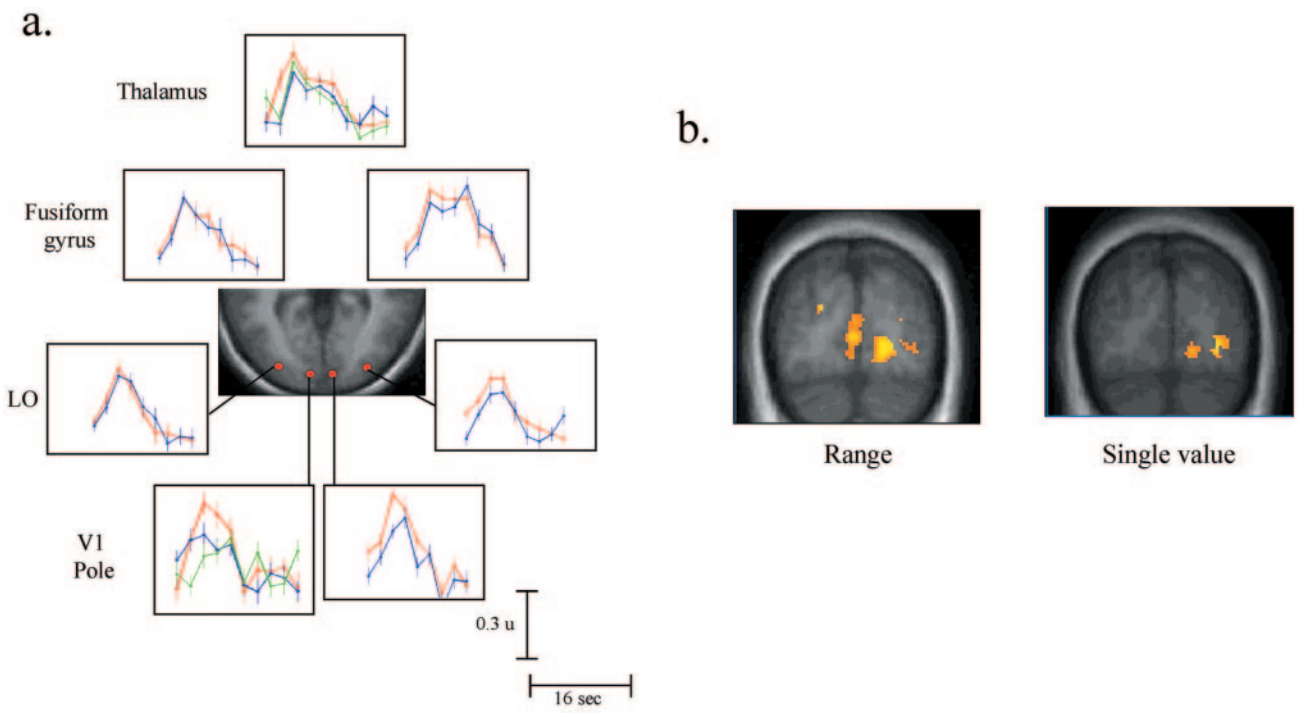

Figure 4. (*a*) Visual activations for V1, LO, fusiform and thalamic regions. The graph for each region shows the haemodynamic response (arbitrary units) associated with Yes (red) and No (blue) trials (±inter-subject standard error). The left of the image is the left of the brain. The visual activations from the subgroup of two subjects who were presented Catch trials (green) are also presented for left V1 and the posterior thalamus. Differential Yes > No responses are shown at the occipital pole. (*b*) Occipital Yes > No activations for threshold stimuli defined by a single value or a range. While right V1 and LO remain differentially activated in the single value model, the loss of statistical power results in the left hemisphere activity failing to reach our threshold of significance.

Occipital Activity and the P100

The onset and offset of a sine wave grating evokes a series of negative and positive waves over occipital and parietal regions, the waveform being dependent on the spatial frequency, extent and location of the grating in the visual field (Kulikowski, 1977; Parker and Salzen, 1982; Plant *et al.*, 1983). At threshold, our gratings were presented for ~50 ms and the resulting EP would therefore have contained contributions from both onset and offset potentials making it difficult to compare directly our waveforms with those evoked in previous studies. However, the waveform and topography of the early part of the response for Yes trials and for high contrast gratings was identical to that found previously for gratings of equivalent spatial frequency (Plant *et al.*, 1983; Kenemans *et al.*, 2000; Martínez *et al.*, 2001; Kenemans *et al.*, 2002). Dipole modelling techniques have suggested that the cortical generators of the early positive wave at 100 ms are located in extra-striate regions on the lateral surface of the occipital lobe (Kenemans *et al.*, 2000; Martínez *et al.*, 2001). Our fMRI results provided some support for a lateral occipital generator in that we found bilateral activations in LO which, in the right hemisphere at least, showed a differential Yes > No response, as found for P100. However, our fMRI analysis also identified V1 and medial occipital foci whose activations were larger than those in LO and whose differential Yes > No responses were bilateral. We therefore used source modelling techniques to establish which of these three candidate regions best accounted for the threshold P100 response. We placed dipole generators bilaterally in V1, LO and medial occipital foci, fixing their locations but allowing their orientations to vary, and compared the measured P100 and its modelled scalp topography (see Fig. 9). In fact, all three regions accounted for more than 83% of the scalp field, with the V1 foci explaining more of the variance than either of the other two candidate generators (V1 85.3%; medial occipital lobe 84.6%; LO 83.6%). Combinations of sources improved the fit. We were thus confronted with several plausible P100 source configurations and, without further evidence, are unable to choose between them. While our results do not help reveal the generator(s) of the threshold P100 we can conclude that activity which correlates with visual consciousness is found in the occipital lobe, 100 ms after the presentation of the stimulus.

Parietal, Limbic and Frontal Cortex and N2, P3 Waves

P3 responses, while typically found in 'oddball' paradigms [see Coles and Rugg (Coles and Rugg, 1995) for review], are also found in signal detection tasks. Hillyard *et al.* (Hillyard *et al.*, 1971) described P3 responses present for Yes trials but not for No trials in an auditory detection paradigm. P3 has an early frontal predominance [P3a (Onofrj *et al.*, 1990)] and is preceded by an N2 wave (Simson *et al.*, 1976, 1977a), both characteristics of the responses found in our study. Our N2 wave (and slow wave response) was left lateralized, which may relate to the high temporal frequency of our brief stimulus presentations (Rebai *et al.*, 1989). Previous fMRI studies have associated P3 waves with activations in the supramarginal gyrus and frontal cortex (Ebmeier *et al.*, 1995; Menon *et al.*, 1997; Opitz *et al.*, 1999). Our fMRI results did not contain parietal or frontal activations, even after lowering our threshold to $P < 0.05$ uncorrected in the fixed effect model. Instead, we found significant suppressions in the posterior cingulate, supramarginal gyrus and frontal regions. The frontal and posterior cingulate fMRI foci showed differential Yes > No suppressions pointing to an association between P3 and fMRI suppressions, a relationship which has been described

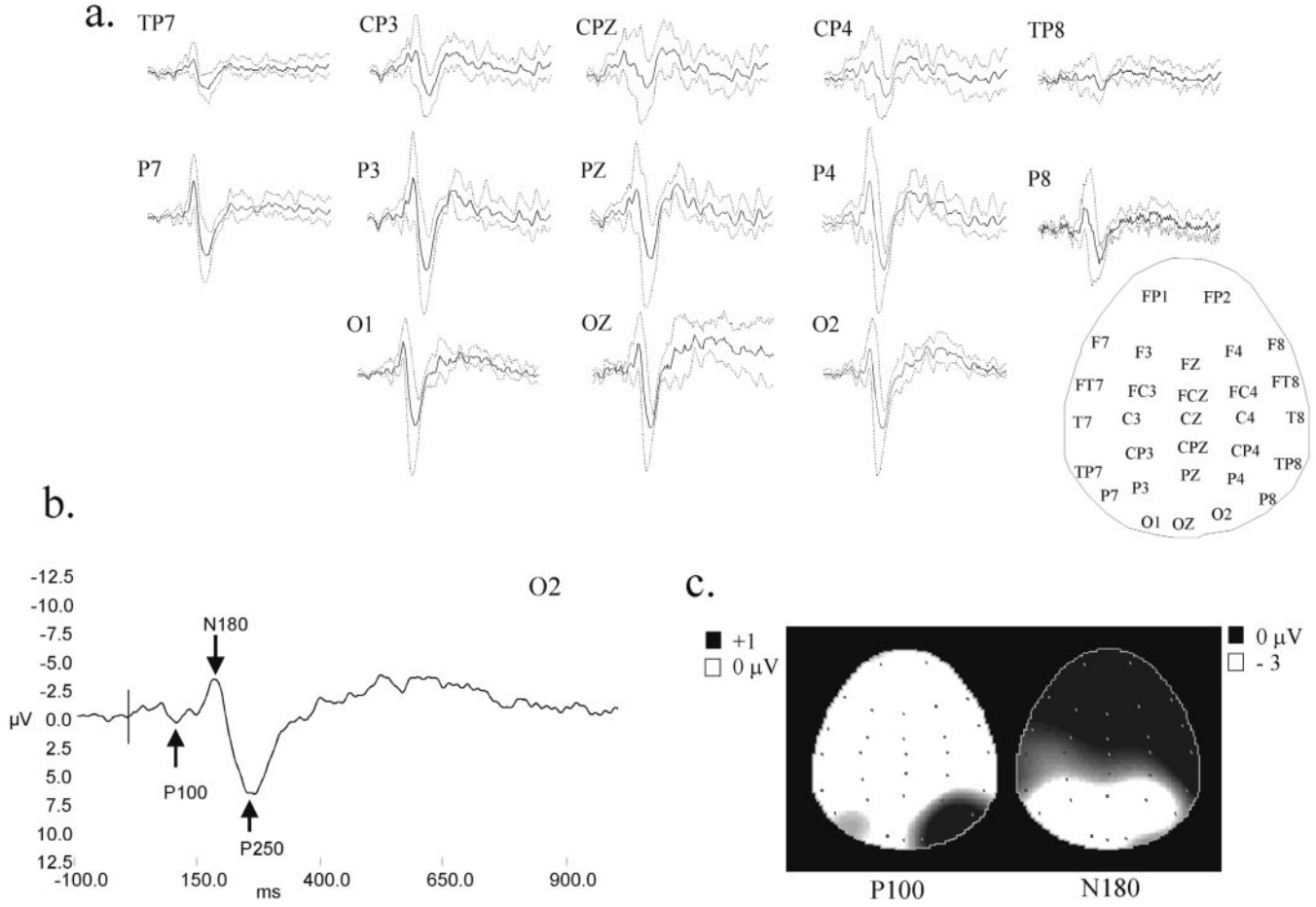

Figure 5. The inter-subject average EP for high contrast gratings. (*a*) The response at each occipital and parietal electrode with the scalp electrode positions given in the inset on the right. Electrodes are arranged as if looking at the head from above (left is left, top is forehead). Mastoid referenced data are shown as occipital electrodes form the posterior boundary of the recording cap, precluding Laplacian transformation. The inter-subject SD of the response is given by the dotted line. (*b*) The response at O2 showing timing and voltage calibrations. The vertical line indicates the onset of the grating. P100, N180 and P250 waves have been marked. (*c*) The scalp topography of P100 and N180 responses. Each dot corresponds to an electrode, the greyscale value relates to the voltage at the given time point.

previously for the posterior cingulate gyrus (Ebmeier *et al.*, 1995). Desmedt and Debecker (Desmedt and Debecker, 1979) hypothesized that P3 relates to the transient inhibition of sustained cortical negativity at task completion, providing a plausible link between P3 and BOLD suppression. However, the model would also predict an increase in BOLD signal related to N2 in P3 generating regions. The fact that we did not find N2-related fMRI activations may reflect the limited temporal resolution of fMRI resulting in a failure to detect activations followed or preceded by more dominant suppressions.

Intracranial recordings have identified multiple P3 generators, including the regions identified in this study – the posterior cingulate, supramarginal gyrus and sub-regions of the frontal lobe (Halgren *et al.*, 1995a,b; Baudena *et al.*, 1995). However, as with the occipital data, our results do not allow us to conclude which regions or combination of regions generates P3 as several source configurations could account for the topography. Whatever the generators, we can conclude that differential processing of Yes and No trials is found in the frontal and parietal/limbic lobes from 260 to 500 ms after the presentation of the stimulus.

Parietal Cortex and the Slow Wave Response

Following P3, a negative slow wave was generated over left parietal and midline electrodes, greater in amplitude for Yes than No trials. The slow wave started after the presentation of the grating and continued until the response button press. One explanation for the wave is that the task had an implicit contingency between the detection of the grating and the response prompt. For visual stimuli, such contingencies elicit CNV (contingent negative variation) O-waves over the parietal lobe (Simson *et al.*, 1977b) which would be present when subjects saw the stimulus and absent when they did not. We do not think the slow wave is related to working memory (Mecklinger and Pfeifer, 1996; McEvoy *et al.*, 1998) as the working memory requirements of our task were minimal. We also do not think the slow wave was a motor preparatory Bereitschaft potential [see Regan (Regan, 1989) for review of pre-motor components] as these are maximal over central, not parietal electrodes.

As described above, we did not find an fMRI activation in the left parietal lobe corresponding to the slow wave topography. We assume that the suppressive fMRI responses in the region obscure fMRI activations. Like the N2 and parietal P3 waves, several source configurations could account for the slow wave activity; however, we can conclude that differential processing of Yes and No trials is found in left parietal/limbic regions from 200 ms before the motor response.

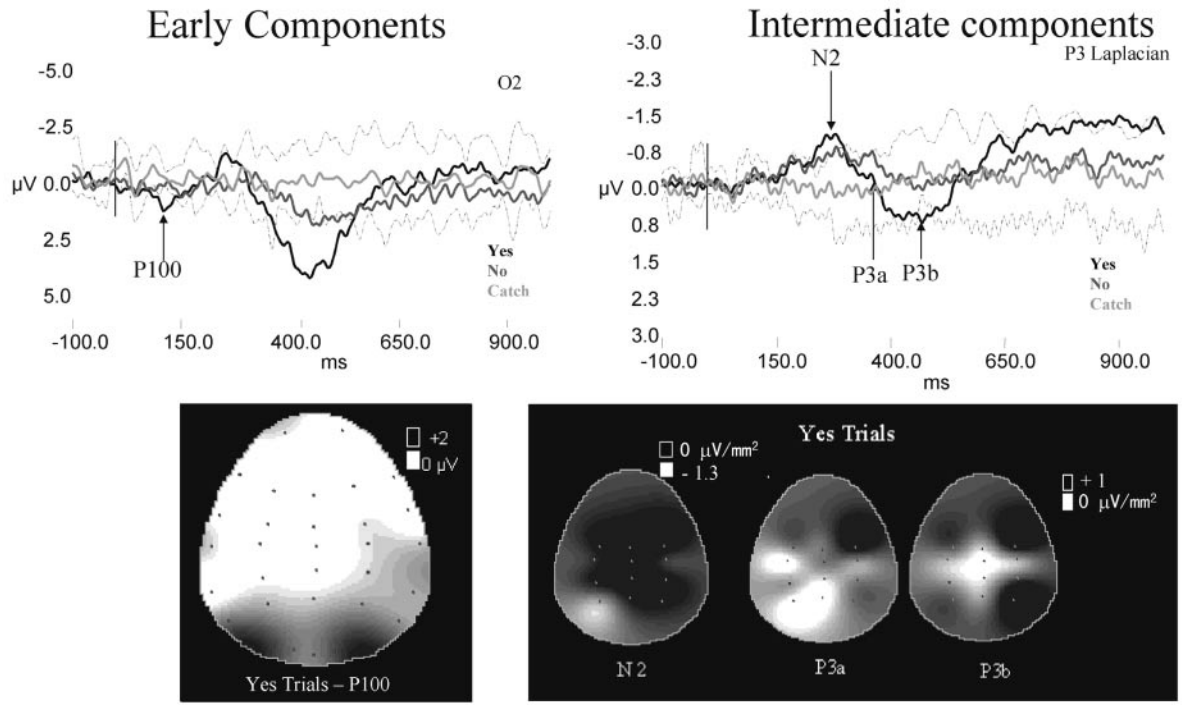

Figure 6. The inter-subject average EPs for threshold gratings. Early latency components are shown on the left (linked mastoid referenced data) with the scalp topography of the threshold P100 wave. Topography conventions as in Figure 5. Yes trials are shown in black, No trials in dark grey, Catch trials in light grey and the inter-subject SD for Catch trials as a dotted line. P100 is of greater amplitude for Yes than No trials. Its topography and waveform is the same at threshold as for the high contrast grating. The right of the figure shows the intermediate latency components: N2, P3a and P3b and their scalp topography. Note that the intermediate latency data have been transformed into its Laplacian derivative, removing the outer electrodes from the montage. N2 is localized to the left parietal region, P3a to bilateral frontal regions and P3b to bilateral parietal regions. N2, P3a and right P3b show significant differential Yes > No responses.

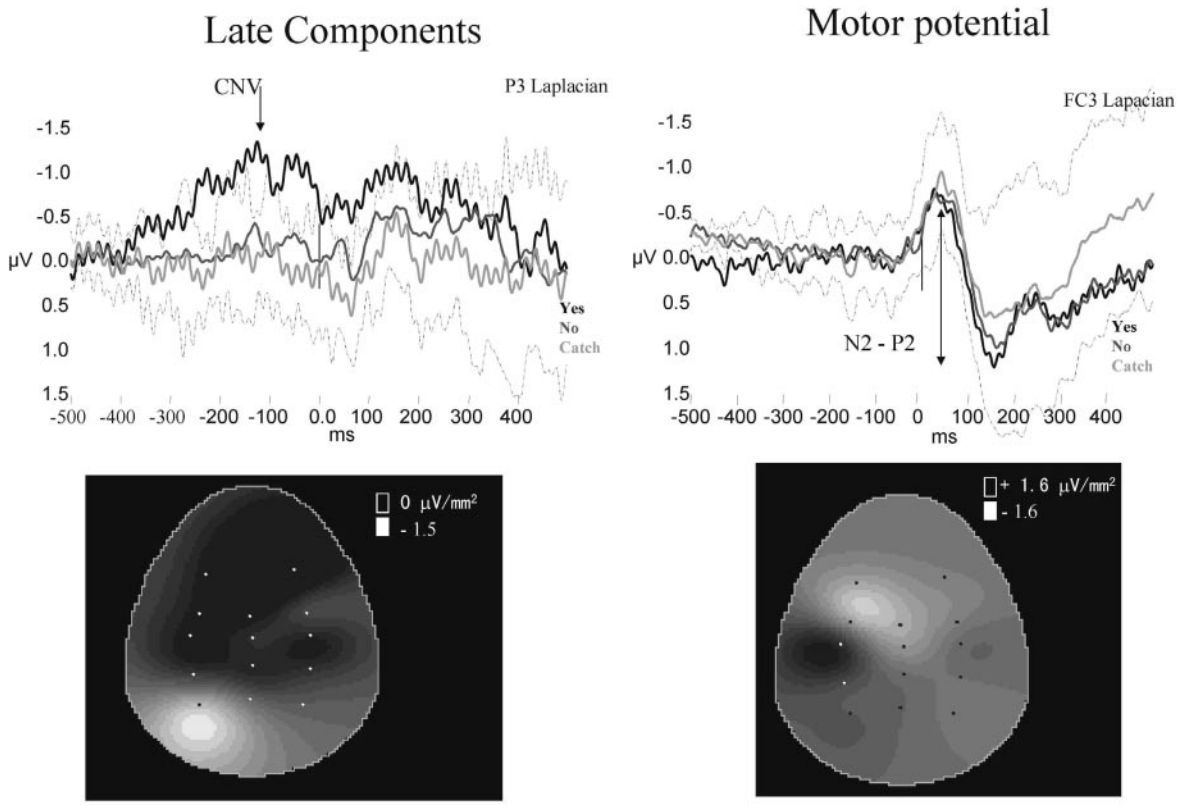

Figure 7. The inter-subject average EPs for late components and motor potentials. Conventions as in Figures 5 and 6. The slow wave scalp map relates to Yes trials at –200 ms, the motor scalp map to P2 in Yes trials. The slow wave is maximal over left parietal cortex. The motor potential is characterized by a tangential dipolar pattern. Both the slow wave and motor potentials exhibit a significant differential response (Yes > No).

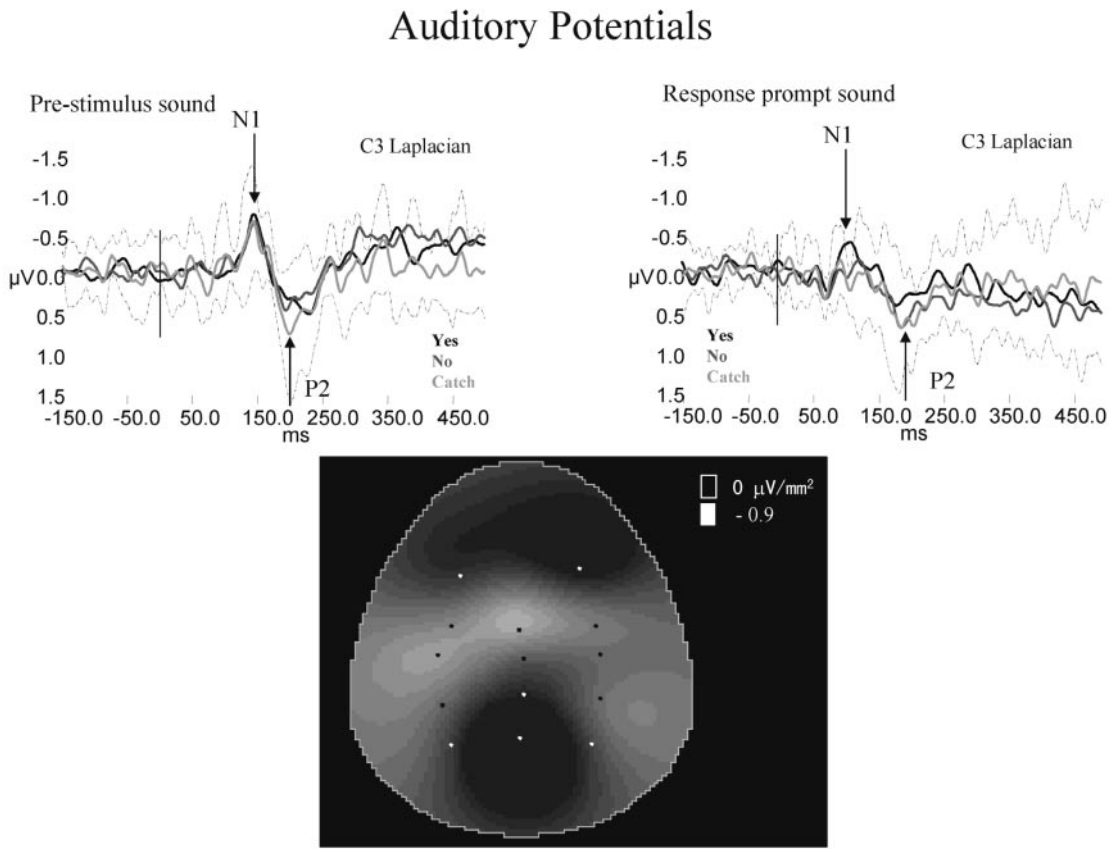

Figure 8. The inter-subject average EPs for sound prompts. The response to the pre-stimulus warning sound is shown on the left, while the response to the response prompt is shown on the right. Conventions as in Figures 5 and 6. The scalp map is of N1 for the warning sound, averaged across Yes, No and Catch trials. Only the second sound shows significant differential N1 activity.

Motor Evoked Responses

The topography of the motor EP co-incident with the button press was consistent with a tangential dipole generator in left sensorimotor cortex. The region was activated in our fMRI study and both EP and fMRI responses were greater for Yes than No trials. The variation in response could not have been caused by differences in the motor representation of index and middle fingers as the Yes and No finger-coding was counter-balanced across subjects. We are not sure why motor cortex was influenced by visual input. As shown in Figure 7, N2/P2 amplitude for No trials was greater than that for Catch trials suggesting an influence of visual input on motor cortex even when subjects had not seen the stimulus.

Auditory Evoked Responses

The latency of auditory N1 and P2 responses for the two sound prompts was different, as would be expected given their differing spectral properties and temporal envelopes [see Naatanen and Picton (Naatanen and Picton, 1987) for a review]. However, the topography of the two components was the same, with maxima at the vertex and temporal electrodes, consistent with the auditory cortex activation found in the fMRI study. The N1 response evoked by the first sound was the same for Yes and No trials. In contrast, N1 evoked by the sound following the grating, was larger for Yes than No trials. The same differential response was seen in our fMRI results in the auditory cortex of the left hemisphere. The N1 augmentation may have been due to an auditory attentional effect, with subjects listening for the second sound more if they had already seen the stimulus and a consequent N1-enhancing processing negativity (Naatanen and Picton, 1987).

Methodological Issues

Before discussing the implications of our findings, we highlight a number of methodological issues. (1) The physiological assumption underlying our integration of EP and fMRI measures is that activation (or suppression) of neural activity within a given cortical region is apparent as: (i) a change in scalp potential (the EP) and (ii) after a delay related to neurovascular coupling, a change in local BOLD contrast (the fMRI response). The integration will fail if an fMRI modulation does not have a corresponding EP or if an EP does not have a corresponding fMRI modulation. Such dissociations occur, for example, when EP generators form closed sources; when fMRI modulations lie within susceptibility artefacts; when one technique is more sensitive than the other; and when EPs are generated through changes in synchronization rather than increases in neuronal activity. The fact that we could identify a differential EP response for the majority of our superficial differential fMRI modulations suggests that such confounds were not compromising integration in this study. (2) Our spatio-temporal description of perceptual processing is necessarily incomplete as our transformation to the Laplacian derivative makes us insensitive to deep brain structures. In particular, we are unable to comment on the timing of correlates of visual consciousness in cerebellar, thalamic, insular and supplementary motor cortex. (3) Our fMRI analysis fits a template haemodynamic response function to the activity at each voxel. If systematic differences in latency or

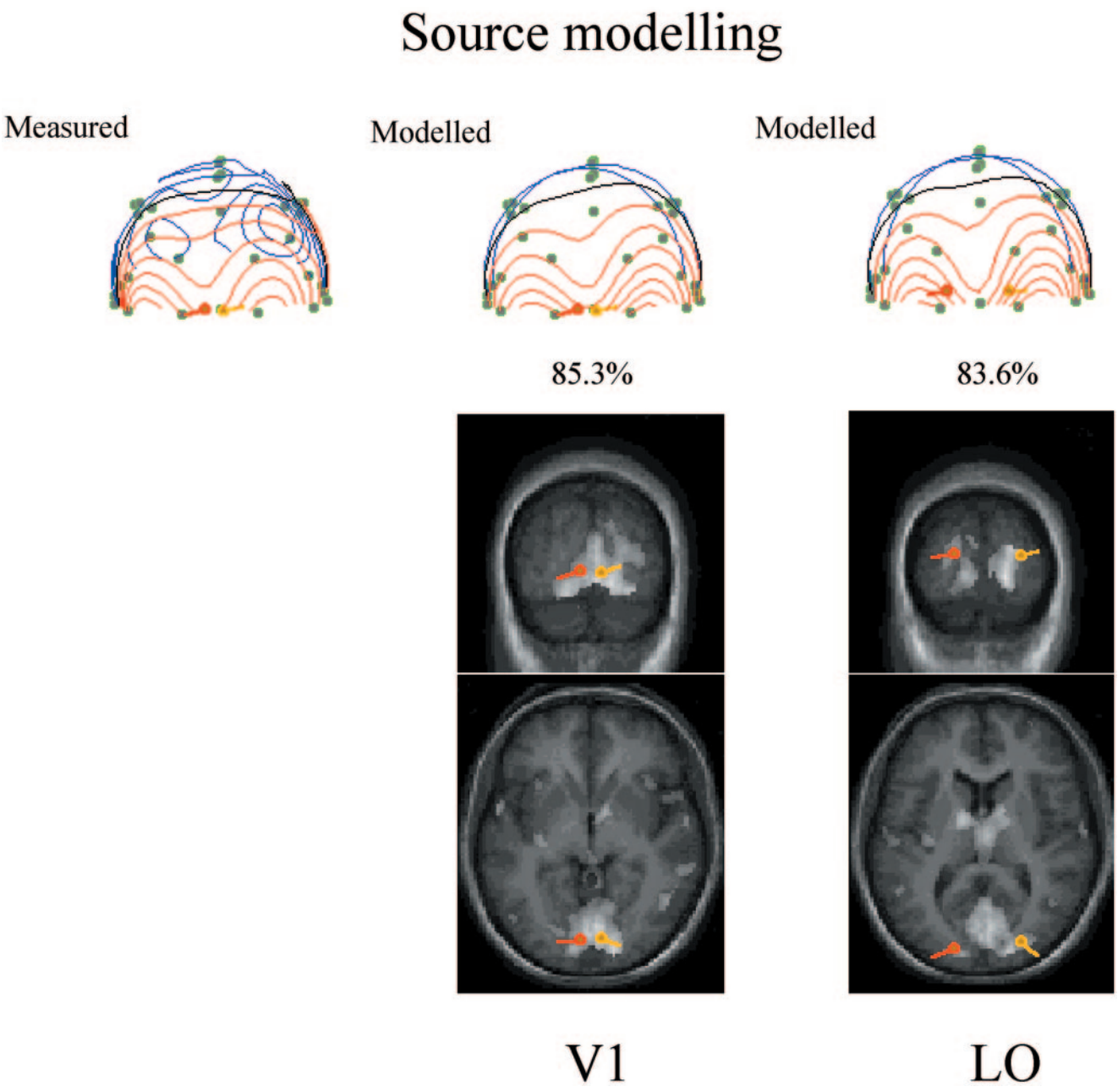

Figure 9. Source modelling. The scalp distribution of the threshold P100 response is shown on the left of the figure presented as a sphere viewed from behind (red = positive; blue = negative scalp potential). The scalp topography of modelled dipole generators placed in V1 and LO are shown on the right (red = left dipole; yellow = right dipole). A coronal and axial slice is shown for each model. The generators have been placed in fMRI activation foci for Yes trials (shown in white) in the sub-group of subjects who took part in the EP experiments. The V1 generators account for the scalp topography better than the LO generators.

response waveform are present for Yes and No trials, the method could find artefactual differences in activity. Figure 4 shows that this was not the case and that haemodynamic responses for different trial categories differ only in their amplitude. (4) Regions with differential No > Yes responses correlate with consciousness, representing areas for which a decrease in activation or suppression is associated with perception. We found two such areas in the fMRI study but no equivalent No > Yes EP responses and are therefore unable to comment on the timing of such activity.

Neural Correlates of Consciousness

The results presented above reveal a sequence of neural activities that meet our operational definition of a correlate of consciousness (a differential response for Yes and No trials). The first correlate of consciousness was found in the occipital lobe at ~100 ms, followed by a left parietal negativity at 260 ms, a parietal and frontal positivity at 300–500 ms and a left parietal slow wave from 200 ms before the motor response. There were also neural correlates of consciousness at the time of the button press and the second sound prompt. Previous studies of conscious vision have arrived at conflicting conclusions as to whether the correlate is localized within individual visual areas (ffytche *et al.*, 1998; Zeki and Bartels, 1998) or distributed across a network of frontal and parietal regions (Lumer *et al.*, 1998; Dehaene *et al.*, 2001). Timing considerations help resolve

the conflict. In our study, a network of regions correlates with consciousness; however, the relative timing of different nodes argues against a unitary process related to the perception of the grating. Instead, it suggests a segregation of function across the network with each node performing a different perceptual/cognitive operation.

Primary Correlates of Conscious Perception

One interpretation of the increment in occipital activity at 100 ms is that it reflects stochastic variations in afferent sensory input. In this model, the occipital activity is pre-conscious with, at a certain level of activation, signals being relayed forward to parietal or frontal areas where, some 160 ms later, the true correlate of consciousness occurs. While plausible, neurobiologically, there are several lines of evidence which suggest that this interpretation is incorrect and that it is the early activity in the occipital lobe which correlates directly with the grating percept. First, is the increasing evidence that, for a given specialized attribute, perceptual and non-perceptual processing is co-localized within the same cortical area (Zeki and ffytche, 1998; ffytche *et al.*, 1998; Moutoussis and Zeki, 2002). This co-localization was first identified in studies of conscious motion vision, where activity in V5 was shown to increase in a motion discrimination task irrespective of whether the stimulus was seen or not. At a constant level of discrimination performance, the only difference between seeing and not seeing motion was the level of activation in V5 (Zeki and ffytche, 1998). No parietal or frontal activity was found to suggest a relay of signals to higher areas, the implication being that conscious motion perception was correlated with activity in motion specialized cortex. Evidence for co-localization in other visual modalities was found in studies of percepts without sensory input (visual hallucinations) (ffytche *et al.*, 1998). Here, a phasic increase in activity within cortex specialized for a given attribute correlated with conscious percepts of that attribute. As for the motion study, no activation was found in parietal or frontal regions, the implication being that the co-localization of conscious and non-conscious perceptual processes generalized to all visual attributes. The conscious percept-related increase in activity within a given cortical area is likely to reflect a change in cortical processing, either through the recruitment of an additional population of cells or modulation of activity within a single population (ffytche, 2000, 2002). Thus it is not all activity within a given area that correlates with consciousness, only some types of activity. Given the evidence for co-localization of conscious and non-conscious perceptual processing in the visual system, it would seem reasonable to assume that perceptual activity for a simple luminance grating would be found in occipital lobe areas involved in the non-conscious processing of such stimuli.

A second line of evidence in favour of a direct occipital correlate of perception is the timing of the activity. Squires *et al.* (Squires *et al.*, 1973) found the auditory N1 wave at 100–170 ms in a signal detection task varied with the confidence of detection, the variation matching that produced by increasing sound intensity. The authors concluded that N1 related to perceptual qualities of the sound such as its loudness or distinctiveness against background noise. A perceptual correlate at 100 ms is also compatible with single cell recordings in the monkey. Super *et al.* (Super *et al.*, 2001) described activity in V1 in a visual detection task which was identical for Yes and No trials before 100 ms but significantly different from 100 ms onwards, although the relationship changed with stimulus saliency. Unlike Super *et al.* (Super *et al.*, 2001) we did not find an EP for Yes or No trials before 100 ms or an EP for No trials after 100 ms, which we attribute to a lack of sensitivity in our threshold EP measurements. However, a V1 response equivalent to that described by Super *et al.* can be inferred from the fact that our fMRI experiment shows activation for No trials (see Fig. 4).

Although not proof of a direct correlate of perception in early occipital areas, our interpretation of the evidence is consistent with the findings of previous studies. Engel *et al.* (Engel *et al.*, 1997) showed that V1 and V2 activity correlated with perceptual thresholds of colour-contrast contour detection while Boynton *et al.* (Boynton *et al.*, 1999) showed an association between psychophysical response functions for contrast increment thresholds and V1, V2 and V3 BOLD signal. Furthermore, in the monkey, behavioural psychometric functions for motion discrimination can be accounted for by the activity of individual cells within motion specialized cortex (Newsome *et al.*, 1989) and micro-stimulation of such cells biases perceptual decision (Salzman *et al.*, 1992).

Our interpretation of the early occipital activity as a direct correlate of perception is further strengthened by evidence against a direct perceptual involvement of the parietal or frontal lobes. Patients with bilateral parietal or frontal lesions, although visually impaired, are nevertheless conscious of the visual attributes they see (Zihl *et al.*, 1983; Castiello *et al.*, 1995).

Perception or Attention

Visual attention can modulate occipital activity as early as 100 ms [see Luck *et al.* (Luck *et al.*, 2000) for review], increasing responses in V1, V2 and V3 for a contrast detection task, irrespective of whether a stimulus is presented or not (Ress *et al.*, 2000). The question thus arises as to whether the increase in occipital activity found in our study relates to attention rather than perception. Could it be that trial-to-trial variations in attention define whether or not a stimulus is perceived? We think not for several reasons. Firstly, the enhancement of EP activity at ~100 ms relates to a 'spotlight' of spatial attention – the direction of attention to a particular location in the visual field. For non-spatial visual attention (e.g. attention to colour) attentional modulations occur much later at ~200 ms (Valdes-Sosa *et al.*, 1998). Since our paradigm did not involve a spatial cue or any trial-to-trial differences in the location of the stimulus, it would seem unlikely that the enhanced occipital activity found at 100 ms was attentional in nature. Secondly, while we found the baseline fMRI response in the absence of a stimulus reported by Ress *et al.* (Ress *et al.*, 2000) (see Catch trial responses in Fig. 4), we also found a differential response for No and Catch trials. If enhanced activity was entirely attributable to visual attention, this would imply that subjects were able to predicted the occurrence of Catch trials, a conclusion that seems unlikely given that they were pseudo-randomly distributed. Thirdly, our crude measure of sustained visual attention, alpha activity during each trial, did not vary for Yes and No trials arguing against a trial-to-trial attentional variation [$t(9) = 0.07$, NS].

Secondary Correlates of Conscious Perception

Parietal, frontal, motor and auditory correlates from 260 to thousands of milliseconds after grating presentation are unlikely to play a role in the same cortical operation as that performed in the occipital lobe at 100 ms. The 160 ms difference in timing, while brief in perceptual terms, is long in neural terms, given that signals are able to reach the cortex within 30 ms of retinal stimulation (ffytche *et al.*, 1995). We would argue that processing in these regions is down-stream of perceptual processing but contingent on its outcome (e.g. listening more for

the second sound after having seen the grating). While we are unsure of the cognitive operations indicated by these secondary correlates, single cell recordings in the monkey parietal region LIP suggest a role for the parietal activity. Shalden and Newsome (Shalden and Newsome, 2001) found neural responses in LIP which were dissociated from both the visual stimulus presented and the subsequent motor action taken. The activity was interpreted as the correlate of the monkey's perceptual decision – processing interposed between the perception of the stimulus and its associated motor response, independent of each operation but carrying the signature of both. The LIP decisional correlate had an onset time of 175 ms and continued until the generation of a response saccade, latencies which bear some resemblance to the timing of our parietal N2 and slow wave activities.

Conclusions

Our results show that activity correlating with consciousness is distributed over time. The broad temporal distribution argues against a unitary, fronto-parietal network correlating with consciousness, suggesting instead a segregation into primary and secondary correlating nodes. Activity in the occipital lobe 100 ms after the presentation of the stimulus is likely to represent a primary correlate of consciousness while activity from 260 ms onwards in parietal, frontal, motor and auditory regions, downstream secondary processes, influenced by earlier perceptual activity but not contributing directly to perception.

Notes

This work was supported by the Wellcome Trust. D.H.ff. is a Wellcome Trust Clinician Scientist Fellow. We wish to thank Oscar García Martín-Prieto and José Antonio Portillo Lozano for programming the stimuli and helping with the EP recordings, and the staff of the neuroimaging unit for help with fMRI acquisition.

Address correspondence to Dr D. ffytche, Institute of Psychiatry, De Crespigny Park, Denmark Hill, London SE5 8AF, UK. Email: d.ffytche@iop.kcl.ac.uk.

References

Baudena P, Halgren E, Heit G, Clarke JM (1995) Intracerebral potentials to rare target and distractor auditory and visual stimuli. III. Frontal cortex. Electroencephalogr Clin Neurophysiol 94:251–264.

Boynton GM, Demb JB, Glover GH, Heeger DJ (1999) Neuronal basis of contrast discrimination. Vision Res 39:257–269.

Castiello U, Scarpa M, Bennett K (1995) A brain-damaged patient with an unusual perceptuomotor deficit. Nature 374:805–808.

Coles MGH, Rugg MD (1995) Event-related brain potentials: an introduction. In: Electrophysiology of mind. Event-related brain potentials and cognition (Rugg MD, Coles MGH, eds), pp. 1–26. Oxford: Oxford University Press.

Crick F, Koch C (1998) Consciousness and neuroscience. Cereb Cortex 8:97–107.

Dehaene S, Naccache L, Cohen L, Bihan DL, Mangin JF, Poline JB, Riviere D (2001) Cerebral mechanisms of word masking and unconscious repetition priming. Nat Neurosci 4:752–758.

Desmedt JE, Debecker J (1979) Wave form and neural mechanism of the decision P350 elicited without pre-stimulus CNV or readiness potential in random sequences of near-threshold auditory clicks and finger stimuli. Electroencephalogr Clin Neurophysiol 47:648–670.

Ebmeier KP, Steele JD, MacKenzie DM, O'Carroll RE, Kydd RR, Glabus MF, Blackwood DH, Rugg MD, Goodwin GM (1995) Cognitive brain potentials and regional cerebral blood flow equivalents during two- and three-sound auditory 'oddball tasks'. Electroencephalogr Clin Neurophysiol 95:434–443.

Engel S, Zhang X, Wandell B (1997) Colour tuning in human visual cortex measured with functional magnetic resonance imaging. Nature 388:68–71.

ffytche DH (2000) Imaging conscious vision. In: Neural correlates of consciousness: empirical and conceptual questions (Metzinger T, ed.), pp. 221–230. Cambridge, MA: MIT Press.

ffytche DH (2002) Neural codes for conscious vision. Trends Cogn Sci 6:493–495.

ffytche DH, Zeki S (1996) Brain activity related to the perception of illusory contours. Neuroimage 3:104–108.

ffytche DH, Guy CN, Zeki S (1995) The parallel visual motion inputs into areas V1 and V5 of human cerebral cortex. Brain 118:1375–1394.

ffytche DH, Howard RJ, Brammer MJ, David A, Woodruff P, Williams S (1998) The anatomy of conscious vision: an fMRI study of visual hallucinations. Nat Neurosci 1:738–742.

Friston KJ, Williams S, Howard R, Frackowiak RS, Turner R (1996a) Movement-related effects in fMRI time-series. Magn Reson Med 35:346–355.

Friston KJ, Holmes A, Poline JB, Price CJ, Frith CD (1996b) Detecting activations in PET and fMRI: levels of inference and power. Neuroimage 4:223–235.

Friston KJ, Holmes AP, Price CJ, Büchel C, Worsley KJ (1999) Multisubject fMRI studies and conjunction analyses. Neuroimage 10:385–396.

Friston KJ, Josephs O, Zarahn E, Holmes AP, Rouquette S, Poline J (2000) To smooth or not to smooth? Bias and efficiency in fMRI time-series analysis. Neuroimage 12:196–208.

Gevins AS (1987) Overview of computer analysis. In: Methods of analysis of brain electrical and magnetic signals: EEG handbook (Gevins AS, Redmond A, eds), pp. 31–83. Amsterdam: Elsevier.

Green DM, Swets JA (1966) Signal detection theory and psychophysics. New York: John Wiley and Sons.

Halgren E, Baudena P, Clarke JM, Heit G, Liegeois C, Chauvel P, Musolino A (1995a) Intracerebral potentials to rare target and distractor auditory and visual stimuli. I. Superior temporal plane and parietal lobe. Electroencephalogr Clin Neurophysiol 94:191–220.

Halgren E, Baudena P, Clarke JM, Heit G, Marinkovic K, Devaux B, Vignal JP, Biraben A (1995b) Intracerebral potentials to rare target and distractor auditory and visual stimuli. II. Medial, lateral and posterior temporal lobe. Electroencephalogr Clin Neurophysiol 94:229–250.

Hillyard SA, Squires KC, Bauer JW, Lindsay PH (1971) Evoked potential correlates of auditory signal detection. Science 172:1357–1360.

Kenemans JL, Baas JMP, Mangun GR, Lijffijt M, Verbaten MN (2000) On the processing of spatial frequencies as revealed by evoked potential source modelling. Clin Neurophysiol 111:1113–1123.

Kenemans JL, Lijffijt M, Camfferman G, Verbaten, MN (2002) Split-second sequential selective activation in human secondary visual cortex. J Cogn Neurosci 14:48–61.

Kulikowski JJ (1977) Separation of occipital potentials related to the detection of pattern and movement. In: Visual evoked potentials in man: new developments (Desmedt JE, ed.), pp. 184–196. Oxford: Clarendon.

Kwong KK, Belliveau JW, Chesler DA, Goldberg IE, Weiskoff RM, Poncelet BP, Kennedy DN, Hoppel BE, Cohen MS, Turner R, Cheng HM, Brady TJ, Rosen BR (1992) Dynamic magnetic resonance imaging of human brain activity during primary sensory stimulation. Proc Natl Acad Sci USA 89:5675–5679.

Levitt H (1971) Transformed up-down methods in psychoacoustics. J Acoustical Soc Am 49:467–477.

Lumer ED, Friston KJ, Rees G (1998) Neural correlates of perceptual rivalry in the human brain. Science 280:1930–1934.

Luck SJ, Woodman GF, Vogel EK (2000) Event-related potential studies of attention. Trends Cogn Sci 4:432–440.

Martínez A, Di Russo F, Anllo-Vento L, Hillyard SA (2001) Electrophysiological analysis of cortical mechanisms of selective attention to high and low spatial frequencies. Clin Neurophysiol 112:1980–1998.

McEvoy LK, Smith ME, Gevins A (1998) Dynamic cortical networks of verbal and spatial working memory: effects of memory load and task practice. Cereb Cortex 8:563–574.

Mecklinger A, Pfeifer E (1996) Event-related potentials reveal topographical and temporal distinct neuronal activation patterns for spatial and object working memory. Cogn Brain Res 4:211–224.

Menon V, Ford JM, Lim KO, Glover GH, Pfefferbaum A (1997) Combined event-related fMRI and EEG evidence for temporal–parietal cortex activation during target detection. Neuroreport 8:3029–3037.

Moutoussis K, Zeki S (2002) The relationship between cortical activation and perception investigated with invisible stimuli. Proc Natl Acad Sci USA 99:9527–9532.

Naatanen R, Picton T (1987) The N1 wave of the human electric and

magnetic response to sound: a review and an analysis of the component structure. Psychophysiology 24:375–425.
Newsome WT, Britten KH, Movshon JA (1989) Neuronal correlates of a perceptual decision. Nature 341:52–54.
Onofrj MC, Ghilardi MF, Fulgente T, Nobilio D, Bazzano S, Ferracci F, Malatesta G (1990) Mapping of event-related potentials to auditory and visual odd-ball paradigms. Electroencephalogr Clin Neurophysiol Suppl 41:183–201.
Opitz B, Mecklinger A, Friederici AD, von Cramon DY (1999) The functional neuroanatomy of novelty processing: integrating ERP and fMRI results. Cereb Cortex 9:379–391.
Parker DM, Salzen EA (1982) Evoked potentials and reaction times to the offset and contrast reversal of sinusoidal gratings. Vision Res 22:205–207.
Plant GT, Zimmern RL, Durden K (1983) Transient visually evoked potentials to the pattern reversal and onset of sinusoidal gratings. Electroencephalogr Clin Neurophysiol 56:147–158.
Rebai M, Mecacci L, Bagot JD, Bonnet C (1989) Influence of spatial frequency and handedness on hemispheric asymmetry in visually steady-state evoked potentials. Neuropsychologia 27:315–324.
Regan D (1989) Human brain electrophysiology: evoked potentials and evoked magnetic fields in science and medicine. New York: Elsevier.
Ress D, Backus BT, Heeger DJ (2000) Activity in primary visual cortex predicts performance in a visual detection task. Nat Neurosci 3:940–945.
Salzman CD, Murasugi CM, Britten KH, Newsome WT (1992) Microstimulation in visual area MT: effects on direction discrimination performance. J Neurosci 12:2331–2355.
Shadlen MN, Newsome WT (2001) Neural basis of a perceptual decision in the parietal cortex (area LIP) of the Rhesus monkey. J Neurophysiol 86:1916–1936.
Simson R, Vaughan HG, Ritter W (1976) The scalp topography of potentials associated with missing visual or auditory stimuli. Electroencephalogr Clin Neurophysiol 40:33–42.
Simson R, Vaughan HG, Ritter W (1977a) The scalp topography of potentials in auditory and visual discrimination tasks. Electroencephalogr Clin Neurophysiol 42:528–535.
Simson R, Vaughan HG, Ritter W (1977b) The scalp topography of potentials in auditory and visual Go/NoGo tasks. Electroencephalogr Clin Neurophysiol 43:864–875.
Squires KC, Hillyard SA, Lindsay PH (1973) Vertex potentials evoked during auditory signal detection: relation to decision criteria. Percept Psychophys 14:265–272.
Super H, Spekreijse H, Lamme VA (2001) Two distinct modes of sensory processing observed in monkey primary visual cortex (V1). Nat Neurosci 4:304–310.
Valdes-Sosa M, Bobes MA, Rodrigues V, Pinilla T (1998) Switching attention without shifting the spotlight: object-based attentional modulation of brain potentials. J Cogn Neurosci 10:137–151.
Zeki S, Bartels A (1998) The asynchrony of consciousness. Proc R Soc Lond B 265:1583–1585.
Zeki S, ffytche DH (1998) The Riddoch syndrome: insights into the neurobiology of conscious vision. Brain 121:25–45.
Zihl J, Von Cramon D, Mai N (1983) Selective disturbance of movement vision after bilateral brain damage. Brain 106:313–340.